Received: 26 June 2019 | Accepted: 19 November 2019

DOI: 10.1096/fba.2019-00053

ORIGINAL ARTICLE

FASEB BioAdvances WILEY

Changes in the R-region interactions depend on phosphorylation and contribute to PKA and PKC regulation of the cystic fibrosis transmembrane conductance regulator chloride channel

Diogo R. Poroca[1] | **Noha Amer**[1] | **Audrey Li**[1] | **John W. Hanrahan**[2] | **Valerie M. Chappe**[1]

[1]Department of Physiology & Biophysics, Dalhousie University, Halifax, NS, Canada

[2]Department of Physiology, McGill University, Montreal, QC, Canada

Correspondence
Valerie Chappe, Faculty of Medicine, Department of Physiology & Biophysics, Dalhousie University, Room 3R1, Sir Charles Tupper Medical Building, 5850 College Street, PO Box 1500, Halifax, Nova Scotia B3H 4R2, Canada.
Email: valerie.chappe@dal.ca

Funding information
NSERC; Nova Scotia Graduate Scholarship and Science Without Borders-Brazil

Abstract

The CFTR chloride channel is regulated by phosphorylation at PKA and PKC consensus sites within its regulatory region (R-region) through a mechanism, which is still not completely understood. We used a split-CFTR construct expressing the N-term-TMD1-NBD1 (Front Half; FH), TMD2-NBD2-C-Term (Back Half; BH), and the R-region as separate polypeptides (Split-R) in BHK cells, to investigate in situ how different phosphorylation conditions affect the R-region interactions with other parts of the protein. In proximity ligation assays, we studied the formation of complexes between the R-region and each half of the Split-CFTR. We found that at basal conditions, the density of complexes formed between the R-region and both halves of the split channel were equal. PKC stimulation alone had no effect, whereas PKA stimulation induced the formation of more complexes between the R-region and both halves compared to basal conditions. Moreover, PKC + PKA stimulation further enhanced the formation of FH-R complexes by 40% from PKA level. In cells expressing the Split-R with the two inhibitory PKC sites on the R-region inactivated (SR-S641A/T682A), density of FH-R complexes was much higher than in Split-R WT expressing cells after PKC or PKC + PKA stimulation. No differences were observed for BH-R complexes measured at all phosphorylation conditions. Since full-length CFTR channels display large functional responses to PKC + PKA in WT and S641A/T682A mutant, we conclude that FH-R interactions are important for CFTR function. Inactivation of consensus PKC site serine 686 (S686A) significantly reduced the basal BH-R interaction and prevented the PKC enhancing effect on CFTR function and FH-R interaction. The phospho-mimetic mutation (S686D) restored basal BH-R interaction and the PKC enhancing effect on CFTR function with enhanced FH-R interaction. As the channel function is mainly stimulated by PKA phosphorylation of the R-region, and this response is known to be enhanced

Abbreviations: BH, Back half; BHK, Baby hamster kidney; cAMP, Cyclic adenosine monophosphate; CF, Cystic fibrosis; CFTR, Cystic fibrosis transmembrane conductance regulator; CTCF, Corrected total cell fluorescence; FH, Front half; FSK, Forskolin; IBMX, Isobutyl methylxanthine; NBD, Nucleotide-binding domain; PKA, Protein kinase A; PKC, Protein kinase C; PLA, Proximity ligation assay; PMA, Phorbol myristate acetate; SR, Split R-region; TMD, Transmembrane domain.

by PKC phosphorylation, our data support a model in which the regulation of CFTR activation results from increased interactions of the R-region with the N-term-TMD1-NBD1. Also, serine S686 was found to be critical for the PKC enhancing effect which requires a permissive BH-R interaction at basal level and increased FH-R interaction after PKC + PKA phosphorylation.

KEYWORDS

CFTR function, PKC enhancing effect, PKC phosphorylation, R-region interactions

1 | INTRODUCTION

The cystic fibrosis transmembrane conductance regulator (CFTR) is a chloride channel that is deficient in patients with cystic fibrosis (CF), a fatal inherited disease prevalent in Caucasians. CFTR is a member of the ATP-binding cassette family of transporters, composed by two transmembrane domains (TMDs) each connected to nucleotide-binding domains (NBDs) that associate to form two halves (TMD1-NBD1 and TMD2-NBD2). Only in CFTR, the two halves are connected by a unique and intrinsically disordered regulatory region (R-region), which contains multiple PKA and PKC phosphorylation consensus sites.[1-3] Opening and closing (gating) of CFTR channels depends on phosphorylation of the R-region by PKA and PKC along with ATP binding and hydrolysis between the NBDs.[1-5]

In contrast to PKA phosphorylation sites, which individually are not essential for CFTR activation,[2,16,17] individual PKC consensus sites within the R-region do modulate CFTR function.[18,19] PKC phosphorylation minimally activates CFTR (5%-10% of the PKA effect) but profoundly enhances PKA-dependent stimulation through unclear mechanisms that include the alteration of domain-domain interactions to render CFTR more sensitive to PKA.[5,18,20,21] Removal of all nine PKC consensus sites (T582, T604, S641, T682, S686, S707, S790, T791, and S809) abolishes the low activity induced by PKC and dramatically decreases activation by PKA, indicating that one or more PKC sites are needed for CFTR activation.[18] By disrupting different subsets of PKC sites, Chappe and colleagues [20] provided evidence of the importance of S686 to regulate CFTR activity and demonstrated that PKC sites S641 and S682 exert inhibitory effects.[19] The demonstration that association of the R-region with the two halves of CFTR is enhanced by PKA phosphorylation [22] but is lost in a mutant R-region lacking its seven PKC sites (R-7CA) [21] suggests that PKC sites are critical for channel function and for phosphorylation-induced R-region interactions.

Intra- and inter-domain interactions are of the utmost importance for the proper function of the CFTR channel. While the interactions between NBDs and TMDs and their role in the structural rearrangements involved in CFTR gating are well known, the mechanism by which the R-region interacts with other domains of the protein to regulate its function is still a matter of debate. Recently, two structures of the full-length CFTR in the dephosphorylated, ATP-free state and two in the phosphorylated, ATP-bound state, were determined. In both zebrafish [6] and human [7] dephosphorylated structures, most of the R-region is missing but parts of its densities appear localized in the cytoplasmic gap between the NBDs and the TMDs' cytoplasmic loops, presumably preventing dimerization of the NBDs. The human structure shows an additional helix, corresponding to residues 825-843 of the R-region, which contains NEG2 (amino acids 817-838), a conserved segment with a negative net charge of −9, involved in the channel regulation by phosphorylation.[8,9] The phosphorylated structures clearly show the conformational changes of TMDs and NBDs. The R-region, however, becomes even more unstructured and is not visible in cryo-EM maps except for a couple of small amorphous densities and a small helix, for which the amino acid sequence could not be assigned, interacting with residues within the cytoplasmic loop 4 (CL4) and the lasso motif.[10,11] The fact that the R-region is mostly missing in all CFTR structures, hinders the identification of the interacting partners of the R-region, an aspect that needs to be explored to further understand the CFTR activation mechanism.

Static CFTR structures provide limited information regarding the mechanisms by which the R-region regulates CFTR function and their dynamics. NMR studies suggest that multiple interactions of the unphosphorylated R-region with both NBD1 and NBD2 block NBD dimerization, and their disruption by phosphorylation allows NBD dimerization and channel gating. PKA phosphorylation dramatically reduced the R-region association with the NBDs while promoting new interactions with the C-terminal tail, leading to a large chemical shift in the R-region.[12,13] Both NMR studies are consistent with the unphosphorylated R-region blocking NBD dimerization as deduced from the recent high-resolution CFTR structures.[6,7,10,11] An alternative hypothesis is that the unphosphorylated R-region interacts directly with the CLs of the TMDs, especially CL3, and these interactions keep the channel in a closed state regardless of NBD dimerization.[9,14,15] This hypothesis is supported by

the position of the new helix described in the human structure between CLs, potentially interacting with CL 3 and 4 and TM12. Parts of the R-region densities were localized nearby NBD1-CL1 and NBD1-CL4 interfaces, where it could possibly interfere with the NBD-TMD communication, preventing gating.[7]

The unstructured nature of the R-region has limited the information provided by CFTR structures and interacting partners of the phosphorylated R-region. The absence of information on the localization of the phosphorylated R-region leads to two hypotheses; first, the R-region is an inhibitory segment that is displaced from its original position when phosphorylated, allowing channel activation [28,36]; second, the R-region plays a dual role in which it inhibits channel activity when unphosphorylated by preventing NBDs dimerization, and stimulates channel activity upon phosphorylation through a conformation shift that permits the formation of new stimulatory interactions with different partners. Biochemical and functional evidence has shown increases in R-region interactions with other CFTR domains after phosphorylation [13,21,22,32] as well as a stimulatory role for the phosphorylated R-region in channel activity, [30,37,38] thus supporting the second hypothesis.

To further explore this idea, in the present study, we have analyzed R-region interactions with a split-CFTR construct (N-terminal-TMD1-NBD1 + TMD2-NBD2-C-tail) inside the cell and examined the effect of CFTR phosphorylation by PKA and PKC in those interactions. The approach presented here, correlating channel function and R-region dynamics in situ, indicates that phosphorylation regulates channel activity by promoting R-region interactions mostly with the N-terminal half of CFTR (Lasso Motif-TMD1-NBD1). Moreover, we propose a model to explain the enhancing effect of PKC, which has been well characterized functionally but not structurally.

2 | MATERIALS AND METHODS

2.1 | Chemicals

MM13-4 and M3A7 mouse monoclonal anti-CFTR antibodies were from Millipore-Sigma. MAB1660 mouse monoclonal anti-CFTR R-region antibody was from R&D Systems. D6W6L rabbit monoclonal anti-R-region antibody was from Cell Signaling Technology. H-182 rabbit and C-19 goat polyclonal anti-CFTR antibodies were from Santa Cruz Biotechnology. Cy5-conjugated, Cy3-conjugated, and peroxidase-conjugated goat anti-mouse secondary IgG antibodies; Alexa Fluor® 488-conjugated and peroxidase-conjugated goat anti-rabbit secondary IgG antibodies and Alexa Fluor® 488-conjugated and peroxidase-conjugated bovine anti-goat secondary IgG antibodies were from Jackson ImmunoResearch Laboratories Clarity™ Western ECL chemiluminescence detection kit was from Bio-Rad. Ponasterone A (PA), Zeocin, and G418 were from Invitrogen; Methotrexate was from Faulding Inc. QIAprep Spin Miniprep Kit was from Qiagen. Quick change II Site-direct mutagenesis kit was from Agilent Technologies. FuGene® HD Transfection Reagent was from Promega. Protease inhibitors were from ThermoFisher Scientific. Vectashield Mounting Medium for Fluorescence was from Vector Laboratories. Duolink® In Situ PLA® Probe Anti-Mouse MINUS, Duolink® In Situ PLA® Probe Anti-Rabbit PLUS, Duolink® In Situ PLA® Probe Anti-Goat PLUS, Duolink® In Situ Detection Reagents Orange, Duolink® In Situ Mounting Medium with DAPI, Duolink® In Situ Wash Buffers, Fluorescence and other chemicals were from Sigma-Aldrich.

2.2 | Split-ΔR and Split-R transfection into Baby Hamster Kidney Cells

Split-ΔR cDNA was constructed and ligated into the pIND vector as described previously.[22,23] Briefly, Split-ΔR cDNA was constructed by replacing the nucleotides that encode the R domain of CFTR (aa 635-836) with an IRES while introducing a stop codon at the 3′ end of the front half and a Kozak consensus for translation initiation of the back half. Wild-type (R-WT) and mutant R-region cDNAs for R-6CA (S641A/T682A/S707A/ S790A/T791A/S809A), R-S686A and R-S641A/T682A and R-S686D were incorporated into the pNUT vector, with the R-WT used as a template. Mutations were confirmed by sequencing. The purification of Split-ΔR (in pIND vector), R-WT, R-6CA, R-S686A, R-S686D, and R-S641A/T682A (in pNUT vector) was performed using the QIAprep Spin Miniprep Kit according to the manufacturer's instructions. Baby Hamster Kidney (BHK-21) cells were cultured in a 35-mm dish until 50%-80% confluency. Plasmid DNA (7.2 μg) from Split-ΔR (in pIND vector) alone or addition to R-WT, R-6CA, R-S641A/T682A, R-S686A, SR-S686D (in pNUT vector) was mixed with 22 μL of FuGENE® HD reagent in sterile water and incubated for 10 minutes at room temperature before adding to the cells according to the manufacturer's instruction. Forty-eight hours post-transfection, adherent cells were harvested and plated at several different dilutions in selective medium that was changed every 3 days. Stable resistant clones were isolated after 14 days and tested for protein expression. Successful co-transfection of pVgRXR + pIND and pNUT vectors into BHK cells and selection using G418 + Zeocin (pVgRXR + Split-ΔR_{pIND}) and methotrexate (RD_{pNUT}) allowed the expression of three polypeptides: the front half (FH; aa 1-634) and the back half (BH; aa 837-1480) from pIND and the R-region (aa 635-836) from pNUT.

2.3 | Cell culture

BHK cells were grown in DMEM/F12 medium containing 5% fetal bovine serum and 1% penicillin-streptomycin at 37°C in 5% CO2. G418 (400 μg/mL) and Zeocin (250 μg/mL) were used to select cells stably expressing the Split-ΔR alone. Cells stably co-expressing Split-ΔR and wild-type or mutant R-regions were selected using the combination of G418, Zeocin, and Methotrexate (500 μmol/L). The expression of Split-ΔR was induced by Ponasterone A (PA, 10 μmol/L), added to the medium 48 hours prior to each assay.

2.4 | Immunoblotting

BHK cells stably expressing Split-ΔR, Split-ΔR/R-WT (SR-WT), SR-6CA, SR-S686A, SR-S686D, or SR-S641A/T682A were induced with PA for 48 hours, then washed three times with ice-cold PBS, harvested by scrapping and lysed on ice with RIPA buffer supplemented with a protease inhibitor cocktail as described previously.[19] After centrifugation, an aliquot of the cell lysate was assayed for protein concentration using the Bradford method. Extracted proteins were subjected to 7.5% (FH and BH) or 12% (R-region) SDS-PAGE and separated proteins were transferred to a nitrocellulose membrane. Monoclonal anti-CFTR antibodies MM13-4, M3A7, or MAB1660 were used to detect the front half, back half, and R-region polypeptides, respectively, and goat anti-mouse secondary antibody conjugated with peroxidase was detected by chemiluminescence. CFTR protein expression in each sample was estimated based on densitometry of Western blots bands measured using the *ImageJ* software (National Institutes of Health; http://rsb.info.nih.gov/ij/).

2.5 | Fluorescence immunostaining

BHK cells stably expressing the Split-ΔR, SR-WT, SR-6CA, SR-S686A, SR-S686D, and SR-S641A/T682A were grown on glass coverslips at low density. The expression of the Split-ΔR was induced by PA (10 μmol/L) for 48 hours. The medium was removed, and cells were washed four times with PBS, then fixed with a 2% paraformaldehyde/PBS mixture for 20 minutes, and then permeabilized with 0.1% TritonX-100/2% BSA in PBS for 45 minutes at room temperature. After the removal of the permeabilization buffer, the cells were incubated overnight with anti-CFTR antibody (MM13-4 or H-182 to detect the FH; M3A7 or C-19 to detect the BH; MAB1660 to detect the R-region) each diluted in 0.1% TritonX-100/0.2% BSA at 4°C. After antibody labeling, the cells were washed three times with PBS/ 0.1% TritonX-100 for 10 minutes, and then incubated in 600 μL of Cy3- or Alexa Fluor® 488-conjugated secondary antibody, diluted in 0.1% TritonX-100/0.2% BSA, for 1 hour at room temperature, protected from light. This was followed by several washes as described above. When a double labeling experiment was required, the cells were incubated with a second anti-CFTR antibody, followed by a second secondary antibody, and a final wash. The coverslips were removed from the dishes, mounted on a glass microscopy slide, sealed, and allowed to dry at room temperature before storage at −20°C. Slides were viewed using a Zeiss LSM 510 Confocal Microscope at the Dalhousie Cellular & Digital Imaging Facility of the Faculty of Medicine (https://medicine.dal.ca/research-dal-med/facilities/cellular-molecular-digital-imaging.html). Negative controls were performed by either immunolabeling non-transfected cells or by omitting the primary antibody.

2.6 | In situ Proximity Ligation Assay

BHK cells expressing Split-ΔR, SR-WT, SR-6CA, SR-S686A, SR-S686D, and SR-S641A/T682A were cultured on glass coverslips at low density. Cells were then induced by PA for 48 hours, and stimulated (or not), at 37°C for 2 hours prior to the assay, with a cAMP cocktail (150 μmol/L CPT-cAMP, 1 mmol/L IBMX, and 10 μmol/L FSK) to activate PKA, with 20 nmol/L PMA to activate PKC, or with a combination of all stimulators to activate both kinases. Assays were performed following the manufacturer's instructions. Briefly, cells were washed three times with PBS and fixed with 2% paraformaldehyde for 20 minutes at room temperature, followed by permeabilization/blocking in 2% BSA diluted in PBS + 0.1% TritonX-100 for 45 minutes at room temperature. The cells were then incubated at 4°C overnight with the two primary antibodies from different host species simultaneously in PBS/0.1% Triton X-100/0.2% BSA. Front half was detected by rabbit polyclonal H-182 antibody (epitope corresponding to amino acids 1-182 at the N-terminus of human CFTR), back half by goat polyclonal C-19 antibody (epitope mapping near the C-terminus of human CFTR), and R-region by mouse monoclonal MAB1660 (epitope predicted to Cys590-Lys830 of beta-galactosidase-coupled CFTR). Specificity and absence of phospho-sensitivity in the detection of the FH and BH was confirmed by immunoblotting and fluorescence immunolabeling (Figure S1). After removing the primary antibodies, cells were washed three times in PBS/0.1% Triton X-100/0.2% BSA for 10 minutes, and then incubated with two Proximity Ligation Assay (PLA) probes (oligonucleotide-tagged secondary antibodies) diluted 1:5 in PBS/0.1% Triton X-100/0.2% BSA for 60 minutes at 37°C. Each PLA probe, containing a PLUS or MINUS version of the oligonucleotide tag, recognizes different species of primary antibody: probe anti-rabbit PLUS (for H-182), anti-mouse

MINUS (for MAB1660), or anti-goat PLUS (for C-19). The cells were then washed twice with PLA wash buffer A and incubated in the ligation mixture for 30 minutes at 37°C, washed again with PLA wash buffer, and then incubated with the amplification mixture containing fluorophore-tagged oligonucleotides that hybridize to the amplification product, for 100 minutes at 37°C, protected from light. After two final 10 minutes washes in PLA wash buffer, cells were mounted on a glass microscopy slide using the Duolink in situ mounting medium with DAPI, sealed, and allowed to dry at room temperature. Slides were later visualized using a Zeiss Axiovert II MOT Fluorescence Microscope using filters 365/420 nm and 546/590 nm for DAPI and PLA orange fluorophore at the Dalhousie Cellular & Digital Imaging Facility of the Faculty of Medicine. For each condition tested, a total of 110-230 cells distributed in a minimum of eight different microscopic fields were measured from at least three independent experiments (using three different cell passages) using high magnification. PLA signal was calculated as "corrected total cell fluorescence" (CTFC), based on the signal intensity and the area of each individual cell, to normalize the distribution of the signal inside cells with different sizes.[24,25] Every cell was delineated at the cell membrane using bright field images, then the area of each cell and the integrated density, as well as three measurements of the surrounding background, were calculated using the *ImageJ* software (National Institutes of Health; http://rsb.info.nih.gov/ij/) (Figure S2). CTCF was calculated as follows: CTCF = integrated density − (area of selected cell × mean density of background).

2.7 | Iodide efflux

BHK cells were cultured to confluence in six-well plates. After removing the culture medium and washing three times with the efflux buffer (136 mmol/L $NaNO_3$, 3 mmol/L KNO_3, 2 mmol/L $Ca(NO_3)_2$, 11 mmol/L glucose, and 20 mmol/L HEPES; pH 7.4), the cells were incubated with the iodide loading buffer (136 mmol/L NaI, 3 mmol/L KNO_3, 2 mmol/L $Ca(NO_3)_2$, 11 mmol/L glucose, and 20 mmol/L HEPES; pH 7.4) at room temperature for 1 hour. Extracellular iodide was removed and replaced three times with fresh efflux buffer. Afterwards, a new aliquot of efflux buffer was added in each well, collected and replaced with fresh efflux buffer, at 1 minutes intervals, over 15 minutes. The three first samples collected were used to establish a stable efflux baseline (time (t) = 1–3 min). When cells were tested for PKA stimulation alone, a cocktail composed of 150 µmol/L CPT-cAMP, 1 mmol/L IBMX and 10 µmol/L FSK was added into the efflux buffer from t = 4 to 15 minutes. When tested for both PKA and PKC stimulations, cells were exposed to 20 nmol/L PMA for 2 hours before stimulation with the PKA cocktail. Iodide concentration (in nmol/mL/min) in each sample collected (t = 1–15 min) was measured by a computer-controlled iodide-sensitive electrode (Thermo Electron) based on a standard curve generated from known iodide concentrations and plotted versus time (Efflux Analysis Software, copyright to F. Chappe & V. Chappe). From these plots, the iodide efflux rate constant k (min^{-1}) was calculated based on Becq et al (2003)[26] (European working group on CFTR expression) for every minute interval. Iodide efflux peaks (maximum efflux rate obtained during stimulation) were compared relative to efflux rates measured under basal conditions (unstimulated cells) or after specific stimulations.

2.8 | Statistical analysis

Results are reported as the mean ± SEM, N = number of independent experiments. Differences were assessed using the Student's t test, with $P < .05$ considered significant.

3 | RESULTS

In previous works using Split-ΔR/R-CFTR constructs, expressing CFTR channels as three separate polypeptides (Nterm-TMD1 + NBD1: FH; R-region: aa 635-836; TMD2 + NBD2-Cterm: BH), for biochemical and functional studies, we have demonstrated the functional re-assembly of the three domains of the channel (FH, BH, and R-region) which displayed the classical functional features of full-length CFTR.[21,22,27-29]

Immunofluorescence localization, chemical cross-linking, cell surface biotinylation, iodide efflux assays, and patch clamping all confirmed that Split-ΔR channels can be functionally expressed at the plasma membrane of mammalian cells. In iodide efflux and patch-clamp experiments, Split-ΔR channels were found to be functional, and in contrast to full-length CFTR, they were constitutively active and did not respond to PKA activation, due to the absence of the R-region, generating an unregulated halide efflux pathway. Their current/voltage relationships were linear with a mean unitary conductance of ~7 pS in symmetric 150 mmol/L chloride solutions. Co-expressing the R-region (previously named R domain) with Split-ΔR partially inhibited the constitutive channel activity and restored its regulation by PKA and PKA + PKC. Compared to full-length wild-type CFTR, a delay of 2-3 min in their response to kinases was measured in iodide efflux assays. The reason for the delayed efflux response may reflect altered gating by re-assembled channels. Regardless, it was thus clearly demonstrated that co-expressing the R-region partially restores phosphorylation-dependent regulation of Split-ΔR channels in vivo.

Here, we re-used the previously characterized Split construct to investigate the modulation of the R-region interactions after PKA and PKC phosphorylation. We also investigated the role of specific PKC consensus sites in phosphorylation-dependent R-region interactions by probing split-CFTR constructs containing different combinations of mutations within the R-region (R-6CA, R-S641A/T682A, R-S686A, and R-S686D; *see methods*). The selection of PKC sites investigated was based on previous studies using Split and full-length CFTR channels.[18,19,21,22]

3.1 | Expression and co-localization of Split-ΔR and Mutant R-regions

Expression of the three CFTR fragments was confirmed by immunoblotting of lysates from cells stably co-expressing Split-ΔR with either WT (SR-WT) or mutated R-regions (R-6CA, R-S641A/T682A, R-S686A, or R-S686D) using antibodies recognizing each of the three polypeptides. Front and back halves of CFTR were detected as a ~62 kDa band by MM13-4 and M3A7 antibodies, respectively. A ~23 kDa band was obtained after exposure of blotting membranes with the anti-CFTR R-region monoclonal antibody MAB1660 (Figure 1A). Expression of the three polypeptides in all mutants was similar to that of SR-WT, except for a lower expression of the FH in the SR-S641A/T682A construct (69% of WT; $P < .001$) and slightly higher expression of the BH in SR-6CA (118% of WT; $P = .045$) (Figure 1B). All antibodies used were tested for specificity in lysates from non-transfected parental BHK cells (BHK-21). The antibody detecting the R-region of CFTR was previously tested for phosphosensitivity and we found that it was able to recognize the unphosphorylated and phosphorylated R-region similarly.[21]

Split-ΔR and R-region co-localization at the cell periphery was assessed by immunofluorescence

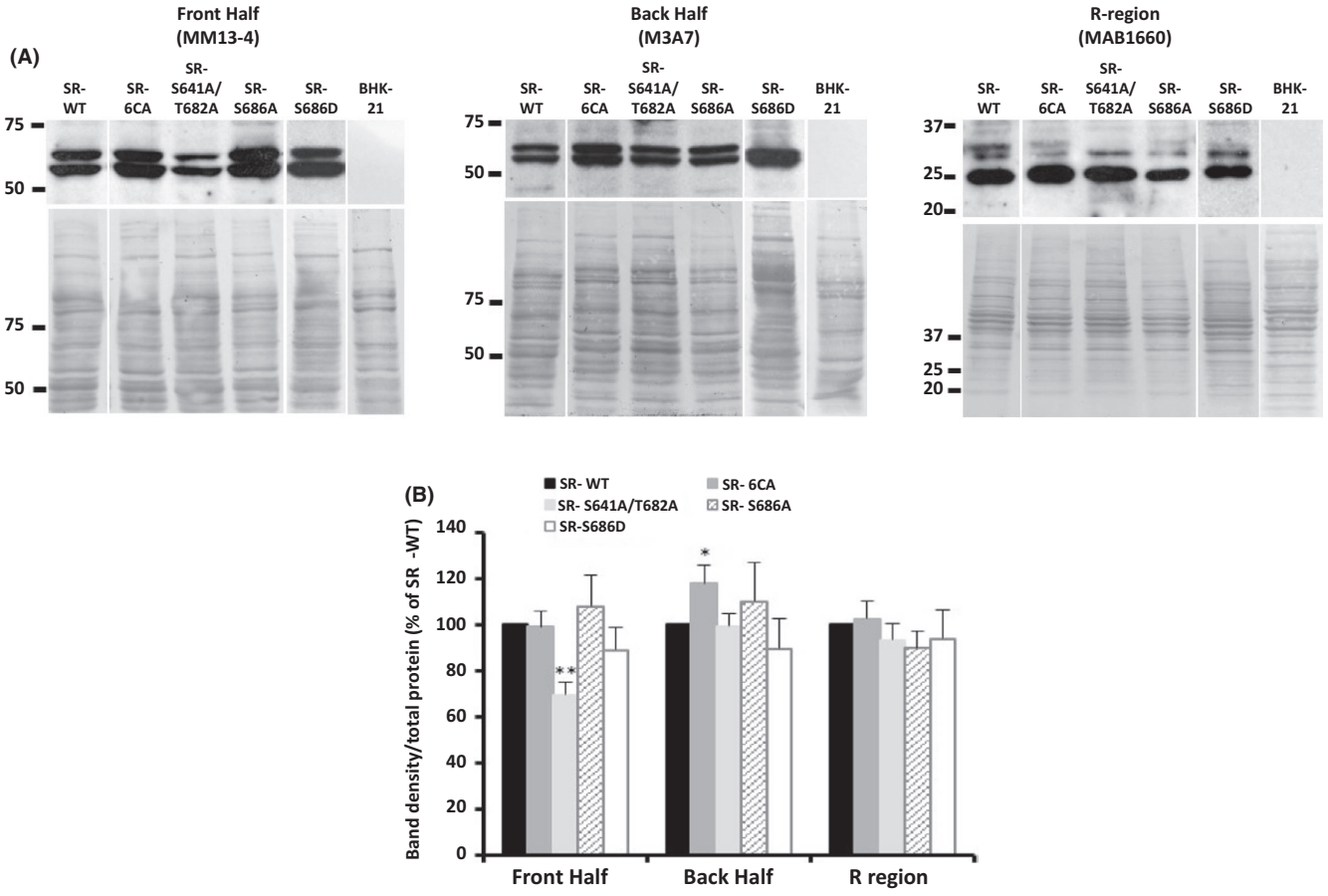

FIGURE 1 Expression of the Split-CFTR front half, back half, and R-region Polypeptides in BHK cells. A. Representative Western blots showing Split-CFTR front half (FH), back half (BH), and R-region in cells expressing SR-WT, SR-6CA, SR-S641A/T682A, SR-S686A, and SR-S686D, detected with MM13-4 (FH), M3A7 (BH), or MAB1660 (R-region) monoclonal antibodies. Negative controls with non-transfected BHK-21 cells probed with each of the antibodies are shown in the far right for each blot. B. Histogram representing averages of band density, normalized to total protein loaded, as measured after membrane staining with amido-black (shown under each blot). All densities were measured using the ImageJ software (National Institutes of Health; http://rsb.info.nih.gov/ij/). Levels for each mutant construct are expressed as a percentage of wild-type. Values are means ± SEM for 3–5 independent experiments; $*P < .05$ and $**P < .001$

labeling with monoclonal antibodies specific for each of the three CFTR polypeptides. Co-localization signals for FH + R-region or BH + R-region of split-ΔR and WT or mutant R-regions were detected with confocal microscopy imaging (Figure 2) for all constructs, consistent with previous results.[22]

3.2 | Co-expressed Split-ΔR and mutant R-regions produce functional channels

We investigated the activity of re-assembled CFTR channels by performing iodide efflux assays using confluent monolayers of BHK cells expressing the Split-ΔR and WT or mutant R-region constructs. The cells were either left untreated (basal) or were pre-treated with PMA to activate PKC for 2 hours prior to the assay. Acute PKA stimulation was achieved with a cAMP cocktail (cpt-cAMP, IBMX, Forskolin; see Section 2) at time $t = 3$ min of the assay. As previously reported,[22,28] cells expressing split-ΔR (no R-region) were unresponsive to cAMP and PMA stimulation as evidenced by the absence of peaks in the iodide efflux traces (Figure 3A). The average basal efflux rate was 0.11 ± 0.01 min^{-1}. As expected, a functional response to kinases stimulation was restored by the co-expression of the split-ΔR and wild-type R-region. A peak in the iodide efflux rate was measured after PKA stimulation (efflux rate at peak $= 0.33 \pm 0.03$ min^{-1}, $P < .001$) (●) and a further increase was measured when cells were pre-treated with PMA prior to PKA stimulation (efflux rate at peak $= 0.60 \pm 0.10$ min^{-1}, $P < .02$) (▲), a mechanism known as the PKC enhancing effect (Figure 3B). Although responsive to PKA and PKC stimulations, split-CFTR channels display delayed and lower efflux peaks when compared to full-length CFTR channels, which was previously thought to reflect a modified gating mechanism in split reassembled channels.[21,22]

All mutant constructs tested were functional with respect to stimulation by the cAMP cocktail, as indicated by the presence of a peak of iodide efflux that was not observed with unstimulated cells (○).

In full-length CFTR channels, S641 and T682 were found to be inhibitory PKC sites conferring a gain of function when mutated to alanine. Also, S686 was found to be necessary and sufficient for the PKC enhancing effect and for CFTR response to phosphorylation.[21,22] Similar to full-length CFTR and cells expressing SR-WT, the PKC enhancing effect was observed after PMA + cAMP stimulation of cells expressing SR-S641A/

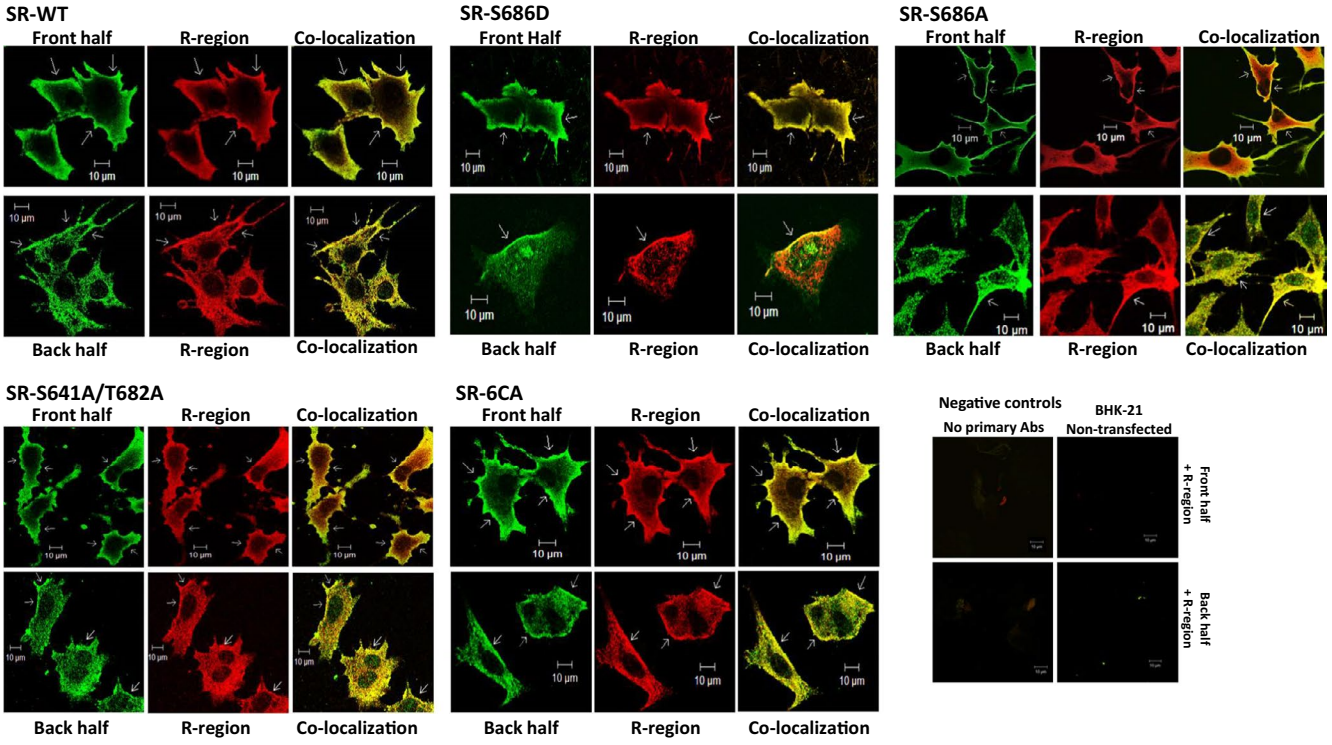

FIGURE 2 Co-localization of Split-CFTR FH, BH, and R-region Polypeptides in BHK cells. Representative confocal microscopy images of BHK cells co-expressing the split-CFTR front half (FH) or back half (BH) in green and the WT or mutant R-regions in red. Upper rows for each construct show FH and R-region co-localization and bottom rows show BH and R-region co-localization in yellow. FH, BH, and R-region were detected by MM13-4, M3A7, and MAB1660 antibodies, respectively. Negative control images where primary antibodies were omitted or where non-transfected BHK cells were used as indicated

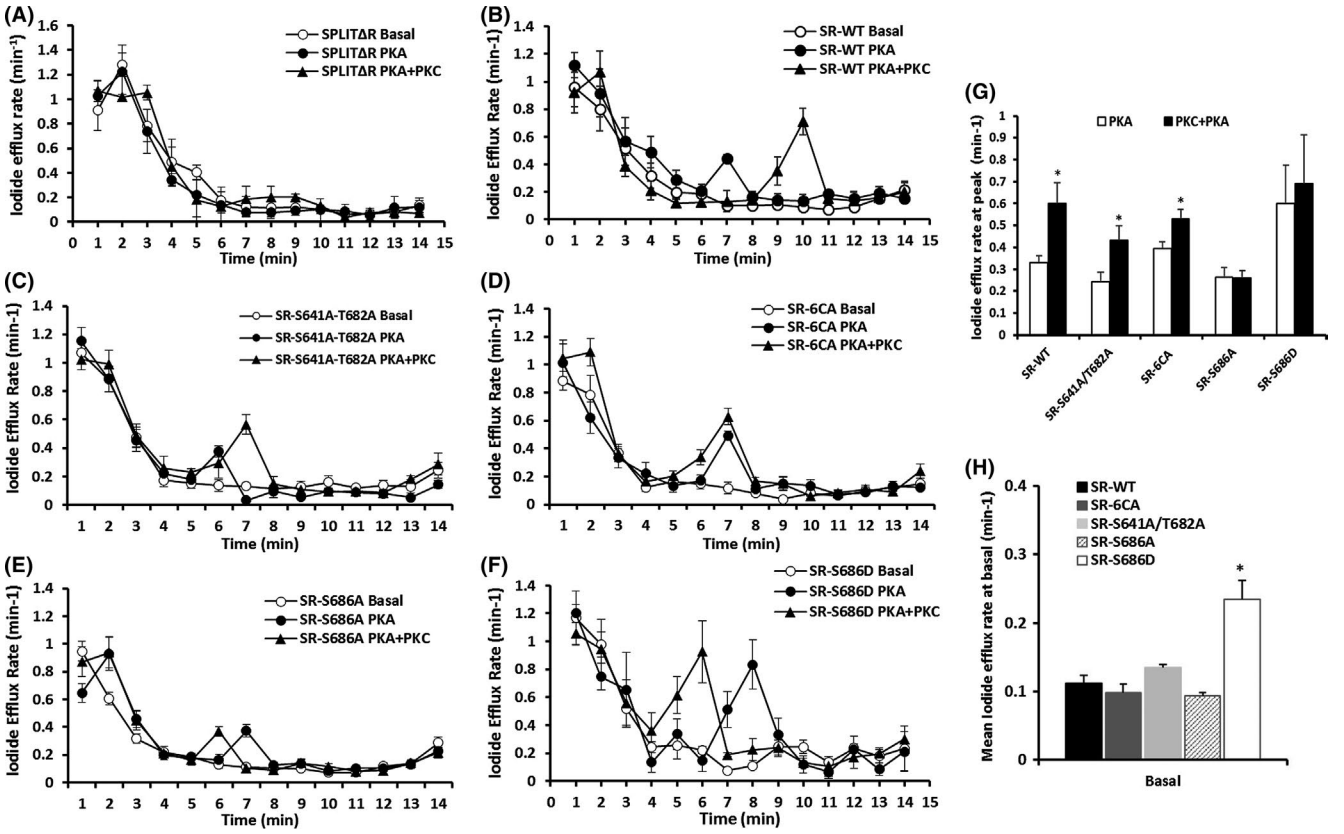

FIGURE 3 Basal and phosphorylation-induced activity of Split-ΔR/R-region constructs. Iodide effluxes were measured in BHK cell monolayers induced with 10 μmol/L ponasterone A (PA) for 48 h before the experiment. A. Iodide efflux traces obtained with cells expressing Split-ΔR CFTR in the absence of the R-region. No peaks were observed after addition of 150 μmol/L CPT-cAMP, 1 mmol/L IBMX, and 10 μmol/L FSK (dark circles) for PKA stimulation or 150 μmol/L CPT-cAMP, 1 mmol/L IBMX ,10 μmol/L FSK, and 20 nmol/L PMA for 2 h prior to the experiments (dark triangles) for PKA + PKC stimulation, starting at time $t = 4$ min. Iodide efflux traces from cells co-expressing Split-ΔR/R-WT (B), R-S641A/T682A (C), R-6CA (D), R-S686A (E), R-S686D (F) with peaks indicating the effect of PKA stimulation (dark circles) or PKC + PKA stimulation (dark triangles). No peak was observed with cells left untreated (basal activity, open circles). G. Iodide efflux rates at peak after PKA and after PKC + PKA stimulation for each of the constructs displayed in A-F. Basal iodide efflux rates were calculated as the average rates from time $t = 4$min to $t = 12$min. Significance (*$P < .05$) was calculated in relation to SR-WT for each condition. Values are means ± SEM of a minimum of four independent experiments performed in duplicate

T682A (Figure 3C) and in cells expressing SR-6CA in which S686 is the only active PKC site (Figure 3D). Peak iodide efflux rates after cAMP and PMA + cAMP stimulation for SR-S641A/T682A were 0.24 ± 0.04 min^{-1} and 0.43 ± 0.07 min^{-1}, respectively, $P < .04$; and for SR-6CA the peak values were 0.39 ± 0.03 and 0.53 ± 0.04, respectively, $P < .03$ (Figure 3G). The slightly higher expression of the BH in SR-6CA and the lower expression of the FH in SR-S641A/T682A did not seem to impact channel responses to phosphorylation.

In contrast, iodide efflux peaks measured in cells expressing SR-S686A (Figure 3E) were not increased by PMA pre-treatment, confirming that the PKC enhancing effect was lost in the absence of S686 (0.26 ± 0.05 min^{-1} for PKA stimulation and 0.26 ± 0.03 min^{-1} for PKC + PKA stimulation; $P > .4$). On the other hand, in cells expressing SR-S686D (Figure 3F), which mimics constitutive phosphorylation of this residue, stimulation with the cAMP cocktail induced very high responses, with iodide efflux peaks that were equivalent to those observed in SR-WT cells after PMA + cAMP treatment (0.60 ± 0.17 min^{-1} for S686D after cAMP and 0.60 ± 0.10 min^{-1} for SR-WT after PMA + cAMP; $P > .5$) (Figure 3G). PMA pre-treatment of SR-S686D-expressing cells did not further increase the iodide efflux rate peak (0.60 ± 0.17 min^{-1} for cAMP and 0.69 ± 0.22 min^{-1} for PMA + cAMP) (Figure 3G), indicating that maximal activity was reached in the absence of PKC activation, suggesting a constitutive enhancing effect (Figure 3F).

Taken together these data show that the three CFTR polypeptides re-assemble into functional Split-R CFTR channels that are responsive to PKA and PKC stimulation. Substituting a phospho-mimetic residue at serine 686 generates channels that reach maximum activation independently of PKC pre-stimulation, further confirming the critical role of S686 in the channel regulation as reported previously with full-length CFTR.[19]

3.3 | Phosphorylation changes the association of the R-region with both halves of CFTR

After confirming that all mutant constructs co-localize at the cell surface and re-assemble into functional CFTR channels capable of phosphorylation-dependent halide ion transport, interaction of the R-region with both CFTR halves was assessed by in situ proximity ligation assays (PLA). For this assay, two primary antibodies, raised in different species, were used to either target FH and R-region or BH and R-region simultaneously. This method enables the identification of interacting proteins. When co-localized within the limit of 40 nm distance (close proximity), two unique complementary DNA strands attached to the secondary antibodies are able to hybridize, circularize, and serve as primers for a rolling circle amplification (PCR reaction) that uses fluorophore-tagged oligonucleotides to generate the fluorescent PLA signal (red dots, Figures 4 and 5). PLA signals were analyzed with the ImageJ software to calculate CFTC for each cell as a measure of the density of complexes formed between the two targeted

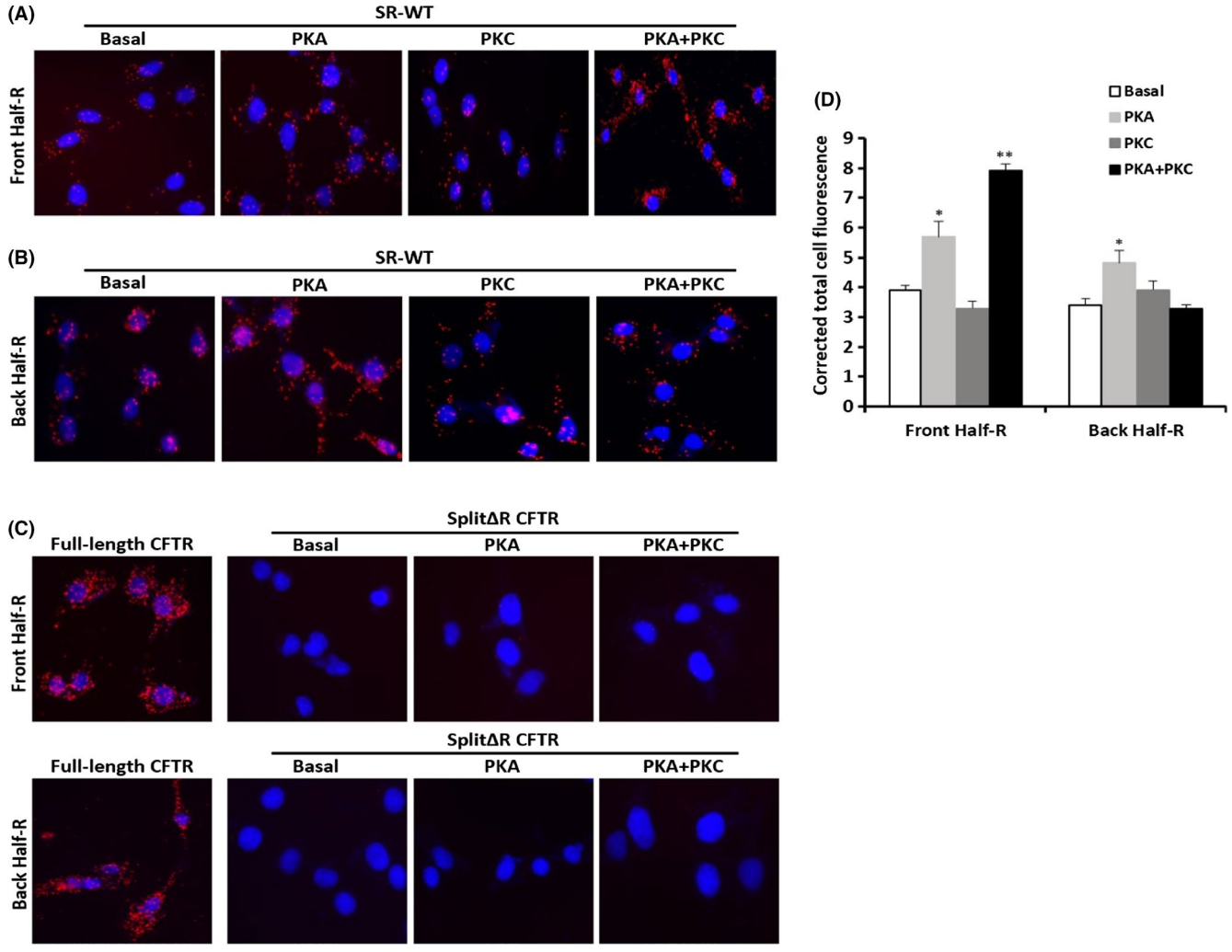

FIGURE 4 R-region Interaction with the FH and the BH of CFTR. Representative fluorescence microscopy images from in situ PLA experiments showing PLA signals for FH-R (A) and the BH-R (B) complexes (red dots) formed at different phosphorylation conditions. SR-WT cells were either left untreated (Basal) or stimulated with 150 µmol/L CPT-cAMP + 1 mmol/L IBMX + 10 µmol/L FSK (PKA), 20 nmol/L PMA for 2 h (PKC), or with 150 µmol/L CPT-cAMP + 1 mmol/L IBMX + 10 µmol/L FSK + 20 nmol/L PMA for 2 h (PKA + PKC). Cells expressing SplitΔR (with no R-region) and full-length CFTR were used as negative and positive controls, respectively. Cell nuclei were stained with DAPI (blue). FH, BH, and R-region were detected by H-182, C-19, and MAB1660 antibodies, respectively. C. In situ PLA experiments in cells expressing full-length CFTR showing positive signals due to the presence of the R-region (positive control), and in cells expressing split-ΔR either untreated or after PKA or PKC stimulation showing negative signals regardless of the phosphorylation condition due to the absence of the R-region (negative control). D. Histogram presenting averages of the corrected total cell fluorescence (CTCF) for the PLA signal for FH-R and BH-R, measured in BHK cells in each condition displayed in A and B (see Section 2 for CTCF calculation). Statistical significance (*$P < .01$; **$P < .001$) was calculated in relation to basal values for each half. Values are means ± SEM for a minimum of five independent experiments

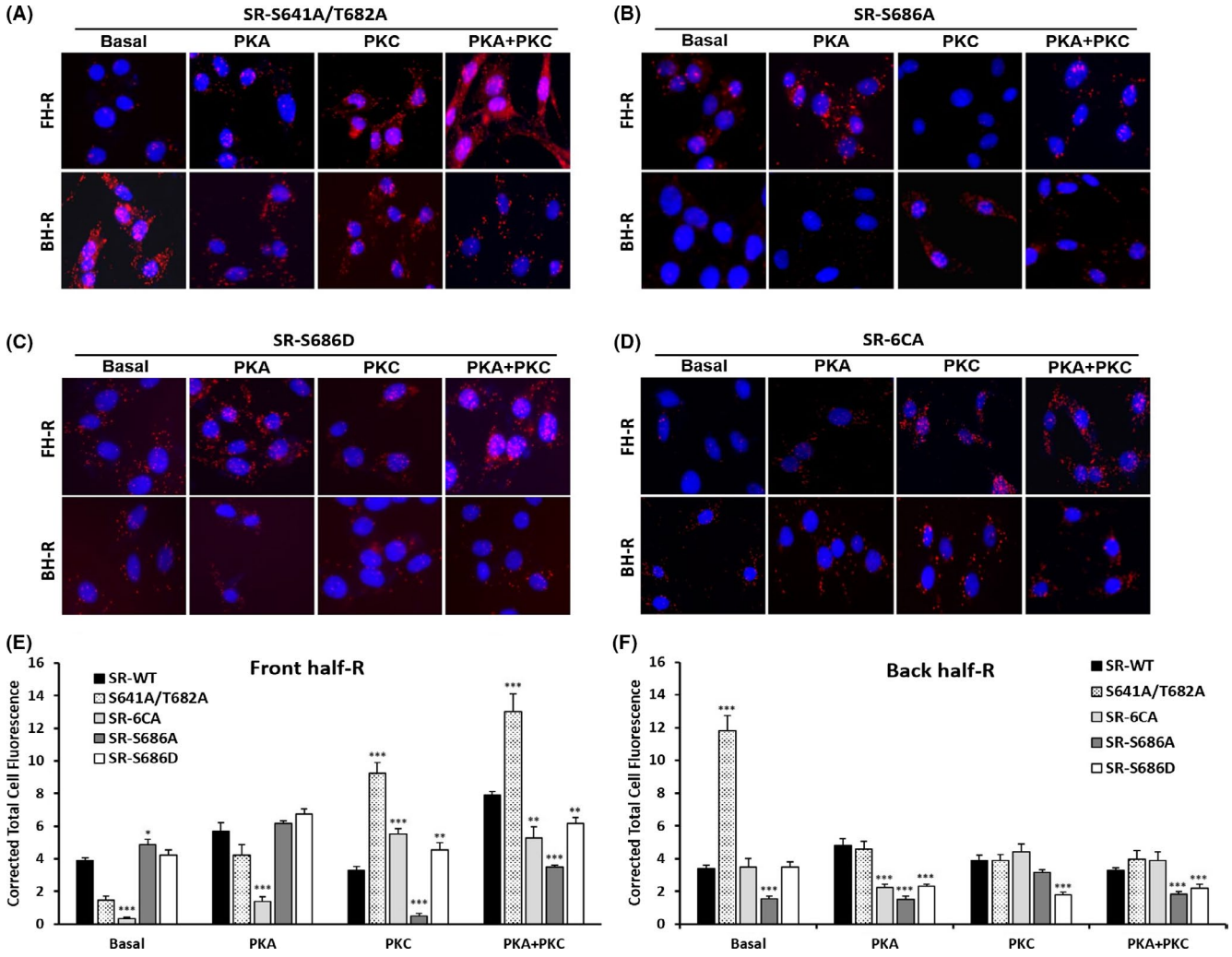

FIGURE 5 Mutant R-region interactions with the FH and the BH of CFTR. Representative fluorescence microscopy images from in situ PLA experiments showing FH-R (upper row) and BH-R (lower row) complexes formed (red dots) for mutant constructs SR-S641A/T682A (A), SR-S686A (B), SR-S686Dm (C), and SR-6CA (D) at basal condition or after PKA or PKA + PKC stimulation as described before. Cell nuclei were stained with DAPI (blue). FH, BH, and R-region were detected by H-182, C-19, and MAB1660 antibodies, respectively. Histograms presenting the average of corrected total cell fluorescence for FH-R (E) and BH-R (F) PLA signals measured in BHK cells from A-D. Statistical significance (*$P < .05$; **$P < .01$; ***$P < .001$) was calculated in relation to values for SR-WT in each phosphorylation condition. Values are means ± SEM for a minimum of 3 + 5 independent experiments

domains (see Section 2 and Figure S2). The use of a Split-CFTR construct expressing the R-region separated from the CFTR halves aimed to simulate intermolecular protein-protein interactions.

The front half (H-182) and back half (C-19) antibodies used in PLA experiments were first tested for specificity and sensitivity by immunofluorescence and immunoblotting. Both antibodies detected the FH and the BH at their expected molecular weight (~ 62kd) and at the cell periphery (Figures 1 and 2; Figure S1) in transfected cells but not in control cells (BHK-21). Anti-R-region antibody MAB1660 was previously tested and recognized the unphosphorylated and phosphorylated versions of the R-region similarly.[21]

We have used H-182 + MAB1660 antibodies to investigate R-region interaction with the FH (FH-R) or C-19 + MAB1660 antibodies to investigate R-region interaction with the BH (BH-R). Negatives controls were performed in BHK cells expressing the Split-ΔR CFTR. As expected, in the absence of the R-region, no PLA signal was observed regardless of the stimulation with PKA and PKA + PKC agonists, confirming the specificity of the signal. In cells transfected with the full-length CFTR (positive control), the presence of the R-region generated strong PLA signals reflecting the presence of the R-region attached to the CFTR halves (Figure 4C).

We first imaged PLA signals in BHK cells stably expressing SR-WT stimulated with either the cAMP cocktail, PMA, PMA + cAMP cocktail, or left untreated (basal) (Figure 4A,B). At basal conditions, with unstimulated cells, the density of interactions between the R-region and both Split-CFTR halves were similar ($P > .1$). In contrast, the

PLA signal increased by 45% from basal condition after cell stimulation with the cAMP cocktail (CTCF = 3.90 ± 0.18 at basal and 5.67 ± 0.55 after cAMP; $P < .01$) and further increased to double of basal (CTCF = 7.91 ± 0.21; $P < .001$) after PMA + cAMP cocktail stimulation. Stimulation with PMA alone did not affect CTCF values, which remained similar to those under basal condition, indicating no changes in FH-R interaction under this condition (Figure 4A,D). In BH-R interaction experiments, the PLA signal was enhanced by 42% when cells were stimulated by the cAMP cocktail (CTCF = 3.41 ± 0.20 at basal to 4.82 ± 0.39 after PKA stimulation; $P < .01$). No changes were found after PMA or PMA + cAMP cocktail treatments (Figure 4B,D).

These results indicate that PKA phosphorylation, which is the major CFTR activator, induces the formation of more complexes between the R-region and both parts (Nterm-TMD1-NBD1: FH; TMD2-NBD2-Cterm: BH) of the split-CFTR channel. Interestingly, maximal activation of CFTR, which is achieved by the PKC enhancing effect of PKA responses, induced the formation of a higher density of complexes, specifically between the R-region and the front half of CFTR (Nterm-TMD1-NBD1), indicating that FH-R interactions are important for channel function (see proposed model in Figure 6).

3.4 | Mutations at consensus PKC sites disturb the R-region interaction with both halves of CFTR

After establishing how the wild-type R-region interactions with both halves of CFTR change depending on its phosphorylation status, we asked whether mutations at PKC sites (R-6CA, R-S641A/T682A, R-S686D, and R-S686A) modify the

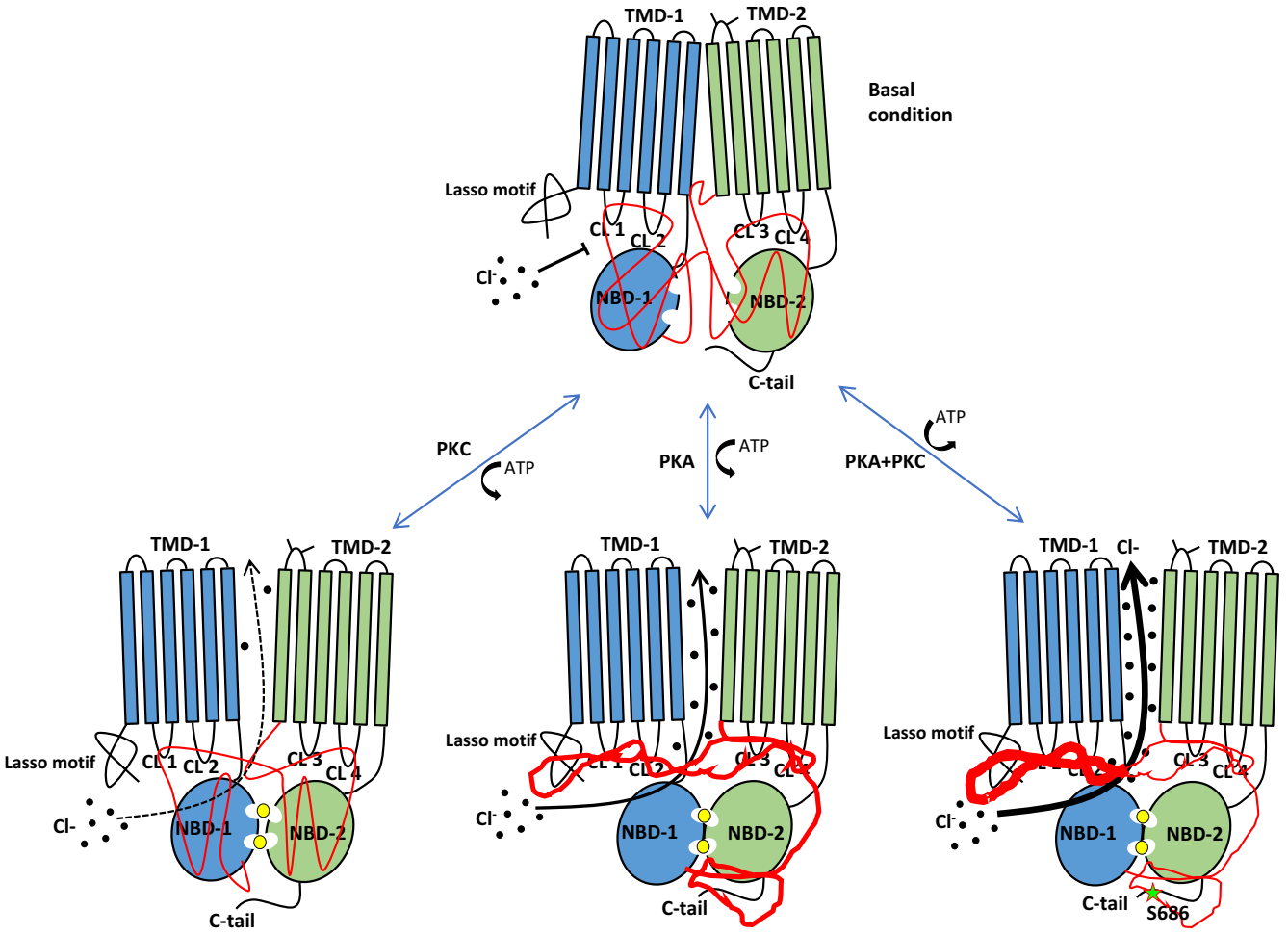

FIGURE 6 Schematic model of the R-region dynamic interactions with the split-CFTR. When the channel is closed, under basal conditions, the R-region interacts equally with both half of the split-CFTR, preventing NBD dimerization. Following PKC phosphorylation, the R-region interaction strength remains unchanged but to a new permissive location allows NBD dimerization, making the split-CFTR channel competent for gating with minimal activity. After PKA phosphorylation, the R-region is removed from the NBDs interface and increases its interactions, mostly with the FH but also with the BH, allowing normal gating and activity of the channel. In the presence of both PKA and PKC phosphorylation, the strongest FH-R interaction is measured, while a basal BH-R interaction enables the enhancing effect of PKC. Black dots: Chloride ions; black arrows: chloride flow; Star indicates the approximate location of S686

R-region dynamics, since PKC mutations are known to affect channel function.

In cells expressing the Split-R CFTR with the two inhibitory PKC sites inactivated (SR-S641A/T682A), under basal conditions, the density of BH-R complexes formed increased by 3.5-fold compared with SR-WT (SR-S641A/T682A CTCF = 11.8 ± 0.91 compared to 3.41 ± 0.20 for SR-WT; $P < .001$), whereas 2.5 fold less FH-R complexes were measured compared to SR-WT (CTCF = 3.90 ± 0.18 for SR-WT and 1.45 ± 0.28 for SR-S641A/T682A; $P < .01$) (Figure 5A,E,F). Although there was a 30% reduced expression of the FH for this construct compared to SR-WT, this cannot account for 2.5-fold reduction in complexes observed but rather indicates a shift of the R-region interaction toward the BH. Nonetheless, this low density in FH-R complexes formed at basal (CTCF = 1.45 ± 0.28) increased after stimulation of PKA (CTCF = 4.24 ± 0.65; $P < .001$), PKC (CTCF = 9.26 ± 0.64; $P < .001$), and PKC + PKA (CTCF = 13.01 ± 1.11; $P < .001$) (Figure 5A,E). Interestingly, all CTCF values were much higher in cells expressing SR-S641A/T682A than in SR WT expressing cells after PKC (3.29 ± 0.24 for SR-WT; $P < .001$) or PKC + PKA (7.91 ± 0.21 for SR-WT; $P < .001$) stimulation (Figure 5E). Regarding BH-R interactions, the density of complexes measured at basal conditions was high compared to SR-WT but remained similar to SR-WT under all phosphorylation conditions (Figure 5F). Since full-length CFTR channels carrying S641A and T682A mutations display larger functional responses to PKA and PKC phosphorylation than WT CFTR,[20] the fact that density of FH-R complexes in SR-S641A/T682A was the highest measured among all constructs after PKC + PKA, reinforces the importance of FH-R interactions for channel function (Figure 6).

In full-length CFTR with the S686A mutation, the functional response to PKA was largely reduced and the enhancing effect of PKC was lost.[20] In the present study, at basal conditions the density of BH-R complexes was low compared to the SR-WT (CTCF = 1.56 ± 0.14; $P < .001$) (Figure 5B,F) while the density of FH-R complexes was higher (CTCF = 4.86 ± 0.35; $P < .05$) (Figure 5B,E), indicating a shift of the R-region. Interestingly, FH-R complexes formed after PKC stimulation were lost with this construct (CTCF = 0.51 ± 0.14 for SR-S686A compared to 3.29 ± 0.24 for SR-WT; $P < .001$) and the density of FH-R complexes measured after PKC + PKA stimulation was half that of SR-WT (CTCF = 3.49 ± 0.13; $P < .001$), suggesting that serine 686 plays a key role in the PKC enhancement of FH-R interactions as observed in SR-WT (Figure 4D).

When testing the functionally opposite mutant construct (S686D), we expected a contrasting result, and this was partially achieved. Unlike S686A, densities of R-region complexes formed with both halves under basal conditions, resembled that of SR-WT, indicating that phosphorylation at this site restores proper basal interaction of the R-region with the BH (Figure 5C,E,F). The density of FH-R complexes measured after PKC stimulation was higher than with the SR-WT (CTCF = 4.54 ± 0.46 for SR-S686D and 3.29 ± 0.24 for SR-WT; $P < .05$). However, the PLA signal for FH-R complexes formation after PKA + PKC stimulation was significantly increased (CTCF = 6.16 ± 0.38; $P < .001$), although still lower than SR-WT (CTCF = 7.91 ± 0.21; $P < .01$). Basal and PKA-induced FH-R interactions seem not to be dependent on S686 phosphorylation as PLA signals remained similar to SR-WT in both S686 mutants (CTCF = 5.67 ± 0.55 for WT, 6.15 ± 0.18 for S686A and 6.75 ± 0.33 for S686D; $P > .1$) (Figure 5C,E). Densities of BH-R complexes measured in SR-S686D remained low compared to SR-WT in all phosphorylation conditions (Figure 5F).

The SR-6CA construct, where Ser686 is the only functional PKC site, induces functional responses to PKA or PKC + PKA stimulation, when measured in iodide efflux assays, similar to the SR-WT, despite lacking six PKC sites (Figure 3D). In this mutant, the PLA signal representing the densities of complexes formed between the FH and R-region under basal conditions was virtually abolished, indicating an almost complete dissociation of the R-region from the FH (<10% of the SR-WT; CTCF = 0.33 ± 0.07 for 6CA and 3.89 ± 0.18 for WT; $P < .001$) while no changes were observed in the densities of BH-R complexes (Figure 5D,E,F). Note that similar to SR-S641A/T682A, the reduced density of FH-R complexes formed under basal conditions did not impact the channel response to the PKC enhancing effect, unlike what we found with reduced BH-R interaction observed in SR-S686A construct, which abolished that response according to the current iodide efflux assays and in previous studies.[19] Although still very low compared to the WT, we measured an increase in the density of FH-R complexes formed after PKA stimulation, as expected for a functional channel (CTCF = 0.33 ± 0.07 at basal and 1.40 ± 0.27 after PKA; $P < .01$). Stimulation of PKC and PKC + PKA strongly increased the density of FH-R complexes compared to basal conditions (CTCF = 5.54 ± 0.31 and 5.28 ± 0.68, respectively; $P < .001$) (Figure 5D,E).

4 | DISCUSSION

Phosphorylation of the R-region-mediated CFTR activation is well established; however, the mechanisms by which it controls channel gating remain to be elucidated. As a disordered segment,[12,13,30,31] the R-region probably exerts its regulation on CFTR function through local conformational shifts induced by phosphorylation, which changes the number and strength of interactions with distinct parts of the channel. Several partners for intramolecular interactions with the R-region, including all other CFTR subdomains,

have been described.[9,12,13,32,33] Homology models of the R-region are not possible because it is unique to CFTR and the attempts to predict its structure using computational methods have led to conflicting results [34,35]; thus, it remains uncertain how the R-region is arranged in the context of the full protein and how it activates CFTR when phosphorylated. Recently, electron cryo-microscopy structures of the full-length CFTR from zebrafish and humans, in both unphosphorylated and phosphorylated states were determined.[6,7,10,11] The two orthologs were found to be very similar, and in the unphosphorylated state, display a mostly disordered R-region positioned between the NBDs and the cytoplasmic loops, making multiple contacts with both halves of the molecule, consistent with our results and model proposed here (Figure 6). In the phosphorylated state,[10,11] the R-region is displaced from between the NBDs and becomes more unstructured and not visible in the Cryo-EM maps except for a small helix and a few amorphous densities. Taking advantage of the Split-R CFTR constructs, where the three generated polypeptides forming the CFTR channel can be considered as separated proteins in these assays, the use of in situ PLA assays allowed us to explore the structural changes triggered by CFTR stimulation by phosphorylation in the native cell environment, showing insightful data on the R-region dynamics upon phosphorylation. In situ PLA signals do not demonstrate direct physical interaction between the two proteins investigated but rather show that two proteins are in close physical proximity and can be considered sufficiently closed to interact. Like other immunoassays, PLA data depend on the quality and optimization of the antibodies used. For our assays, we carefully tested several antibodies for their specificity and phospho-sensitivity, and only the more suitable antibodies were selected and optimized to meet the requirements of the assay (see Figure S1). PLA assays eventually generate false-positive signals due to nonspecific antibody binding, that is, to a very abundant or by the random, fortuitous proximity of two proteins that hardly establish direct interaction. To mitigate this, PLA assays using SplitΔR-CFTR (R-region absent) were performed in parallel for all experiments, and so that signals measured in those cells could be subtracted from the signal measured in cells expressing the R-region. On the other hand, false-negative results could arise due to steric hindrance. Formation of the protein complex may promote conformational changes that partially occlude the epitope that is recognized by one or both antibodies, preventing detection of the complex and generation of PLA signals. In this study, we have not encountered any situation where the formation of complexes between the R-region and the other parts of CFTR was lost.

In PLA assays, we found that in cells at basal conditions (no stimulation), the R-region similarly interacts with both CFTR halves of the inactive channel, consistent with previous studies.[6,7,9,12-14,33] This association under basal conditions probably reflects R-region interactions with both NBDs, keeping the channel in the closed state by preventing dimerization. Upon PKA phosphorylation of the R-region, we observed a significant increase in the density of PLA signals for both FH-R and BH-R complexes, reflecting a stronger association of the R-region with other parts of the protein, as previously reported[21,22] (Figure 6).

Although in vitro NMR studies using a shorter R-region construct have shown a drastic reduction in the R-region interaction with NBD1 (part of our FH construct) after PKA phosphorylation,[12,13] a well conserved, highly charged segment comprising the second helix of the lasso motif (amino acids 46-60) has been shown to interact with the R-region after PKA phosphorylation.[32] The successive elimination of acidic residues within the second lasso motif helix was shown to gradually reduce both channel activity and binding to the R-region. This segment is implied to modulate channel function through interactions with the R-region[32] and constitutes a good candidate for an interacting partner of the PKA-phosphorylated R-region, contributing to the stronger FH-R signal detected here. In addition to the lasso motif, the human CFTR structure in the PKA phosphorylated state shows amorphous densities of the R-region, likely interacting to the outside face of NBD1.[11] In similar NMR studies,[13] PKA phosphorylation was found to reduce interaction of the R-region with NBD2 while enhancing its interaction with the C-terminal tail of CFTR (part of our BH construct; aa 1438-1480). The interaction with the C-terminal tail induced an important chemical shift perturbation of the R-region suggesting its involvement in channel activation.[13] In the present work, a significant increase in the BH-R interaction was also observed after PKA stimulation. Our data thus support the notion that phosphorylation leads to displacement of the R-region from the NBDs interface to other CFTR regions, possibly N- and C-terminal ends, where their binding causes stimulatory effects.

We also tested the effect of combining PKA and PKC stimulations on the R-region interactions and measured enhanced density of complexes formed between the R-region to the FH while leaving the formation of complexes with the BH unaltered, indicating that more complexes were formed. The PLA signal for density of R-region complexes formed with the FH induced by PKC + PKA stimulation was twofold higher than under basal conditions and nearly 40% higher than PKA alone. Since addition of PKC nearly doubles CFTR channel functional responses to PKA,[3,4,18] we suggest that novel R-region interactions with the FH support the PKC enhancing effect on channel activity.

In our model, PKC phosphorylation alone did not change the pattern observed under basal conditions, consistent with circular dichroism measurements using recombinant R-region indicating that only PKA and not

PKC phosphorylation induces significant conformational changes[39] and with functional studies showing only minor current activation by PKC alone.[3,4,18] This pattern differs from previous immunoprecipitation experiments that showed an increased R-region binding other parts of CFTR after stimulation by PKC alone.[21] However, those co-immunoprecipitation experiments required cell lysis and protein purification steps that may affect interactions later probed in a non-native, lipid-free, and detergent-containing environment. The PLA assays used in the present study analyzed protein associations in situ (ie, in intact cells) while preserving the membrane environment. In addition, it is a more sensitive and specific technique for evaluating the rapid and transient interactions expected with disordered proteins like the R-region of CFTR. Unphosphorylated R-region was not detected in pull downs with the two halves[21] although substantial interactions with both NBDs have been reported.[12,13] Those interactions were now detected with in situ PLA experiments in which basal conditions reflect the steady-state level of protein phosphorylation in the cell for non-functional channels.

Mutating potential PKC sites was previously shown to modify the CFTR response to phosphorylation by PKA, PKC, and PKC + PKA in both full-length and split-CFTR channels, indicating they have an important functional role.[19,21] This raised the question whether disabling PKC sites would also affect the profile of R-region interactions. Indeed, association of the R-region was lost in co-immunoprecipitation experiments using an R-region lacking all seven PKC sites.[21] We therefore examined the impact of PKC mutations in situ. Among the four constructs studied here, SR-S686D and SR-S641A/T682A can be classified as "gain of function" mutations and SR-S686A as a "loss of function" mutation. We compared PLA signals from SR-S641A/T682A, SR-S686D, and SR-S686A with the ones observed in the SR-WT and SR-6CA, a mutant construct with similar function to the SR-WT despite the lack of six out of seven PKC sites (S686 is the only active site). Under basal conditions, a low density of FH-R complexes was observed in SR-S641A/T682A and SR-6CA channels, which did not prevent their response to phosphorylation. The increasing density of FH-R complexes formed after PKC and PKC + PKA stimulations in SR-S641A/T682A further support that interactions of the phosphorylated R-region with the FH are important to channel activation. In contrast, diminished density of BH-R complexes, under basal conditions, observed in SR-S686A channels could reflect the inability of this mutant R-region to form more interactions with the FH after PKC + PKA phosphorylation, abolishing the PKC enhancing effect. On the other hand, construct with the opposite mutation S686D, BH-R formed complexes with similar density to WT R-region, and FH-R interactions responded to phosphorylation. These results suggest that interactions of the R-region, at basal conditions, with the BH are crucial for the phosphorylation-induced increased interaction with the FH, resulting in channel activation by PKA and PKC enhancing effect. Our data demonstrate that strong anchoring of the unphosphorylated R-region to specific, not yet identified, regions in the BH is critical for R-region phosphorylation-dependent interaction with the FH, which regulates CFTR activity. Basal interactions of the R-region with the FH probably reflect NBD1-R binding and might be related to the inhibitory role attributed to the unphosphorylated R-region, reflecting basal conditions on the cell.[12,13,22,38]

In conclusion, the present work provides the first detailed study of R-region dynamics in situ by examining its association with the FH and BH of CFTR under three stimulatory conditions (PKA, PKC, and PKC + PKA). It shows that R-region associations change considerably depending on phosphorylation states and this mobility likely contributes to kinase regulation of CFTR. The molecular model proposed here shows the FH of CFTR to be the major recipient area for the phosphorylated R-region, promoting channel activation. Moreover, the PKC enhancing effect, characterized by strong FH-R interactions, appears to be mediated by a permissive interaction of the R-region with the BH.

Together with previous results reported by our group,[19,21,22] the present findings reinforce the importance of PKC sites in CFTR function and domain interactions. Here, we highlight serine 686 as a critical site for the PKC enhancing effect, which promotes maximal channel activation. The specific interaction sites in each of the CFTR halves still need to be discovered; however, the comprehension of how phosphorylation changes the R-region dynamics in the context of the full CFTR protein, in its native membrane environment, is of fundamental importance to understand the mechanism by which phosphorylation regulates CFTR activation.

ACKNOWLEDGEMENTS

The authors sincerely thank Frederic Chappe (Dalhousie University) for general technical support and specific training with cell culture and iodide efflux; Stephen Whitefield (CMDI, Dalhousie Faculty of Medicine) for technical support, training and expertise with fluorescence and confocal microscopy; Alexandra Evagelidis (McGill University) for inserting mutations in the R-region constructs; Dr Yassine El Hiani (Dalhousie University) for critical reading of the manuscript and helpful discussions on CFTR structure/function relationship.

This work was supported by NSERC Discovery grant to VC, Nova Scotia Graduate Scholarship and Science Without Borders, Brazil scholarship to DP.

CONFLICT OF INTEREST

There are no conflict of interest to declare.

AUTHOR CONTRIBUTIONS

VM Chappe designed the research, supervised the work, analyzed the data, and revised the manuscript; DR Poroca, N. Amer, and A. Li performed research experiments and analyzed the data; DR Poroca also wrote the paper; JWH supervised the molecular constructs development and revised the manuscript.

REFERENCES

1. Riordan JR, Rommens JM, Kerem BS, et al. Identification of the cystic fibrosis gene: cloning and characterization of complementary DNA. *Science*. 1989;245(4922):1066-1073.
2. Cheng SH, Gregory RJ, Marshall J, et al. Defective intracellular transport and processing of CFTR is the molecular basis of most cystic fibrosis. *Cell*. 1990;63(4):827-834.
3. Berger HA, Travis SM, Welsh MJ. Regulation of the cystic fibrosis transmembrane conductance regulator Cl-channel by specific protein kinases and protein phosphatases. *J Biol Chem*. 1993;268(3):2037-2047.
4. Tabcharani JA, Chang XB, Riordan JR, Hanrahan JW. Phosphorylation-regulated CI− channel in CHO cells stably expressing the cystic fibrosis gene. *Nature*. 1991;352(6336):628.
5. Picciotto MR, Cohn JA, Bertuzzi G, Greengard P, Nairn AC. Phosphorylation of the cystic fibrosis transmembrane conductance regulator. *J Biol Chem*. 1992;267(18):12742-12752.
6. Zhang Z, Chen J. Atomic structure of the cystic fibrosis transmembrane conductance regulator. *Cell*. 2016;167(6):1586-1597.
7. Liu F, Zhang Z, Csanády L, Gadsby DC, Chen J. Molecular structure of the human CFTR ion channel. *Cell*. 2017;169(1):85-95.
8. Xie J, Adams LM, Zhao J, Gerken TA, Davis PB, Ma J. A short segment of the R domain of cystic fibrosis transmembrane conductance regulator contains channel stimulatory and inhibitory activities that are separable by sequence modification. *J Biol Chem*. 2002;277(25):23019-23027.
9. Wang G, Duan DD. Regulation of activation and processing of the cystic fibrosis transmembrane conductance regulator (CFTR) by a complex electrostatic interaction between the regulatory domain and cytoplasmic loop 3. *J Biol Chem*. 2012;287(48):40484-40492.
10. Zhang Z, Liu F, Chen J. Conformational changes of CFTR upon phosphorylation and ATP binding. *Cell*. 2017;170(3):483-491.
11. Zhang Z, Liu F, Chen J. Molecular structure of the ATP-bound, phosphorylated human CFTR. *Proc Natl Acad Sci USA*. 2018;115(50):12757-12762.
12. Baker JM, Hudson RP, Kanelis V, et al. CFTR regulatory region interacts with NBD1 predominantly via multiple transient helices. *Nat Struct Mol Biol*. 2007;14(8):738-745.
13. Bozoky Z, Krzeminski M, Muhandiram R, et al. Regulatory R region of the CFTR chloride channel is a dynamic integrator of phospho-dependent intra-and intermolecular interactions. *Proc Natl Acad Sci USA*. 2013;110(47):E4427-E4436.
14. Wang G. State-dependent regulation of cystic fibrosis transmembrane conductance regulator (CFTR) gating by a high affinity Fe3+ bridge between the regulatory domain and cytoplasmic loop 3. *J Biol Chem*. 2010;285(52):40438-40447.
15. Wang G. The inhibition mechanism of non-phosphorylated Ser768 in the regulatory domain of cystic fibrosis transmembrane conductance regulator. *J Biol Chem*. 2011;286(3):2171-2182.
16. Chang XB, Tabcharani JA, Hou YX, et al. Protein kinase A (PKA) still activates CFTR chloride channel after mutagenesis of all 10 PKA consensus phosphorylation sites. *J Biol Chem*. 1993;268(15):11304-11311.
17. Rich DP, Berger HA, Cheng SH, et al. Regulation of the cystic fibrosis transmembrane conductance regulator Cl-channel by negative charge in the R domain. *J Biol Chem*. 1993;268(27):20259-20267.
18. Chappe V, Hinkson DA, Zhu T, Chang XB, Riordan JR, Hanrahan JW. Phosphorylation of protein kinase C sites in NBD1 and the R domain control CFTR channel activation by PKA. *J Physiol*. 2003;548(1):39-52.
19. Chappe V, Hinkson DA, Howell LD, et al. Stimulatory and inhibitory protein kinase C consensus sequences regulate the cystic fibrosis transmembrane conductance regulator. *Proc Natl Acad Sci USA*. 2004;101(1):390-395.
20. Jia Y, Mathews CJ, Hanrahan JW. Phosphorylation by protein kinase C is required for acute activation of cystic fibrosis transmembrane conductance regulator by protein kinase A. *J Biol Chem*. 1997;272(8):4978-4984.
21. Seavilleklein G, Amer N, Evagelidis A, et al. PKC phosphorylation modulates PKA-dependent binding of the R domain to other domains of CFTR. *Amer J Physiol-Cell Physiol*. 2008;295(5):C1366-C1375.
22. Chappe V, Irvine T, Liao J, Evagelidis A, Hanrahan JW. Phosphorylation of CFTR by PKA promotes binding of the regulatory domain. *EMBO J*. 2005;24(15):2730-2740.
23. Irvine T. Studies of split R domain deleted CFTR channels expressed in mammalian cells. M.Sc Thesis, McGill University, Montreal QC; 2002.
24. Gavet O, Pines J. Progressive activation of CyclinB1-Cdk1 coordinates entry to mitosis. *Dev Cell*. 2010;18(4):533-543.
25. McCloy RA, et al. Partial inhibition of Cdk1 in G2 phase overrides the SAC and decouples mitotic events. *Cell Cycle*. 2014;13(9):1400-1412.
26. Becq F, Auzanneau C, Norez C, Dérand R, Bulteau-Pignoux L. Radiotracer flux method to study CFTR channel activity: regulation, pharmacology and drug discovery. *European Working Group on CFTR Expression D*. 2003;5:1-13.
27. Ostedgaard LS, Rich DP, DeBerg LG, Welsh MJ. Association of domains within the cystic fibrosis transmembrane conductance regulator. *Biochemistry*. 1997;36(6):1287-1294.
28. Csanády L, Chan KW, Seto-Young D, Kopsco DC, Nairn AC, Gadsby DC. Severed channels probe regulation of gating of cystic fibrosis transmembrane conductance regulator by its cytoplasmic domains. *J Gen Physiol*. 2000;116(3):477-500.
29. Chan KW, Csanády L, Seto-Young D, Nairn AC, Gadsby DC. Severed molecules functionally define the boundaries of the cystic fibrosis transmembrane conductance regulator's NH_2-terminal nucleotide binding domain. *J Gen Physiol*. 2000;116(2):163-180.
30. Ostedgaard LS, Baldursson O, Vermeer DW, Welsh MJ, Robertson AD. A functional R domain from cystic fibrosis transmembrane conductance regulator is predominantly unstructured in solution. *Proc Natl Acad Sci USA*. 2000;97(10):5657-5662.
31. Marasini C, Galeno L, Moran O. A SAXS-based ensemble model of the native and phosphorylated regulatory domain of the CFTR. *Cell Mol Life Sci*. 2013;70(5):923-933.
32. Naren AP, Cormet-Boyaka E, Fu J, et al. CFTR chloride channel regulation by an interdomain interaction. *Science*. 1999;286(5439):544-548.

33. Wang W, He Z, O'Shaughnessy TJ, Rux J, Reenstra WW. Domain-domain associations in cystic fibrosis transmembrane conductance regulator. *Amer J Physiol-Cell Physiol*. 2002;282(5):C1170-C1180.
34. Hegedűs T, Serohijos AW, Dokholyan NV, He L, Riordan JR. Computational studies reveal phosphorylation-dependent changes in the unstructured R domain of CFTR. *J Mol Biol*. 2008;378(5):1052-1063.
35. Mornon JP, Lehn P, Callebaut I. Molecular models of the open and closed states of the whole human CFTR protein. *Cell Mol Life Sci*. 2009;66(21):3469-3486.
36. Rich DP, Gregory RJ, Anderson MP, Manavalan P, Smith AE, Welsh MJ. Effect of deleting the R domain on CFTR-generated chloride channels. *Science*. 1991;253(5016):205-207.
37. Winter MC, Welsh MJ. Stimulation of CFTR activity by its phosphorylated R domain. *Nature*. 1997;389(6648):294.
38. Ma J, Zhao J, Drumm ML, Xie J, Davis PB. Function of the R domain in the cystic fibrosis transmembrane conductance regulator chloride channel. *J Biol Chem*. 1997;272(44):28133-28141.
39. Dulhanty AM, Riordan JR. Phosphorylation by cAMP-dependent protein kinase causes a conformational change in the R domain of the cystic fibrosis transmembrane conductance regulator. *Biochemistry*. 1994;33(13):4072-4079.

SUPPORTING INFORMATION

Additional supporting information may be found online in the Supporting Information section.

How to cite this article: Poroca DR, Amer N, Li A, Hanrahan J, Chappe VM. Changes in the R-region interactions depend on phosphorylation and contribute to PKA and PKC regulation of the cystic fibrosis transmembrane conductance regulator chloride channel. *FASEB BioAdvances*. 2020;2:33–48. https://doi.org/10.1096/fba.2019-00053